

Electronic Supplementary Information

Synthesis and Characterisation of Polycarbonates from Spent Lithium Battery Electrolytes

Haiyue Wang^{1†}, Lili Deng^{1†}, Bing Fang¹, Xiaolong Li¹, Liying Guo^{1,*}, Rongrong Zheng¹

(¹ School of Materials Science and Engineering, Shenyang University of Technology,
Shenyang 111003, China)

The supporting information includes thirteen pages and fifteen figures.

General Information

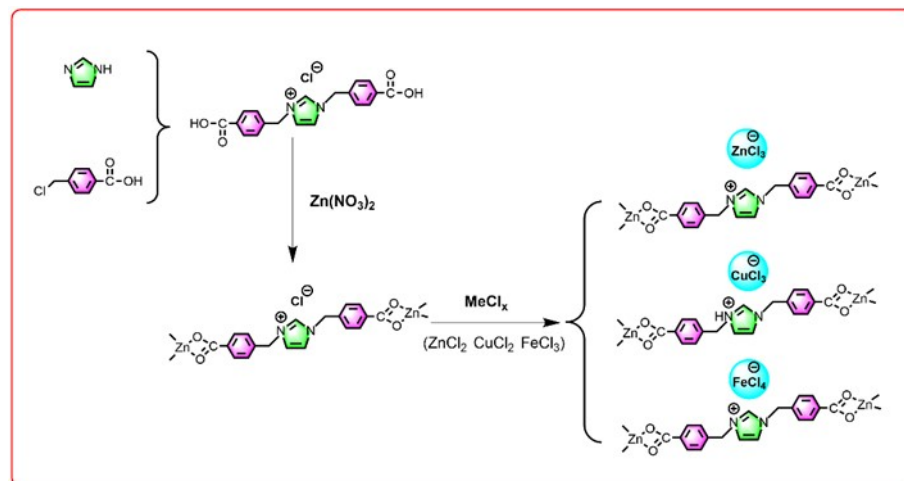


Fig. S1 Reaction process diagram of ILs catalyst

X-Ray Energy Spectrum Analyzer (XFlash 630M), Bruker, Germany, point scanning analysis (depth of about 1 μm), acceleration voltage of 0 ~ 20 keV ; X-ray diffractometer (ULTIMA) was used. The operating voltage was 45 kV, the current was 40 mA, the anode target material was Cu target, K α ray radiation, the scanning angle range was 10-80°, and the scanning speed was 5°/min.



Fig. S2. X-Ray Energy Spectrum Analyzer of catalysis.

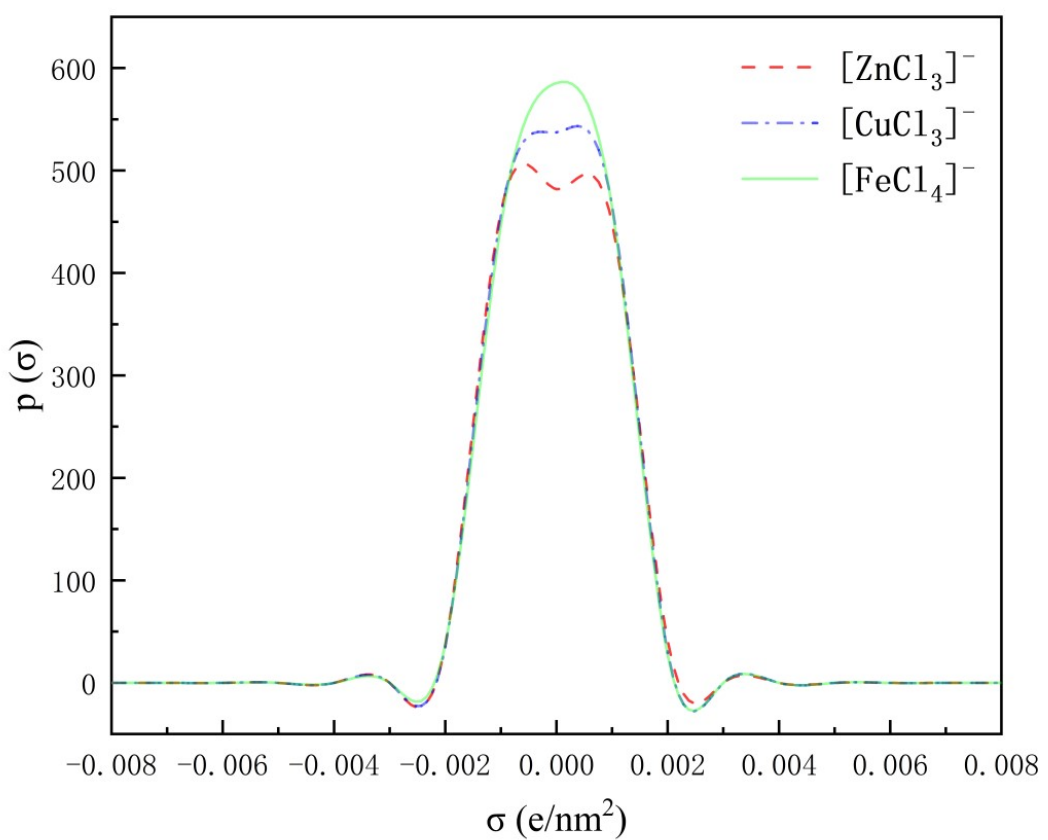


Fig. S3. Sigma-profile of the functionalized cation computed by COSMO-MS.

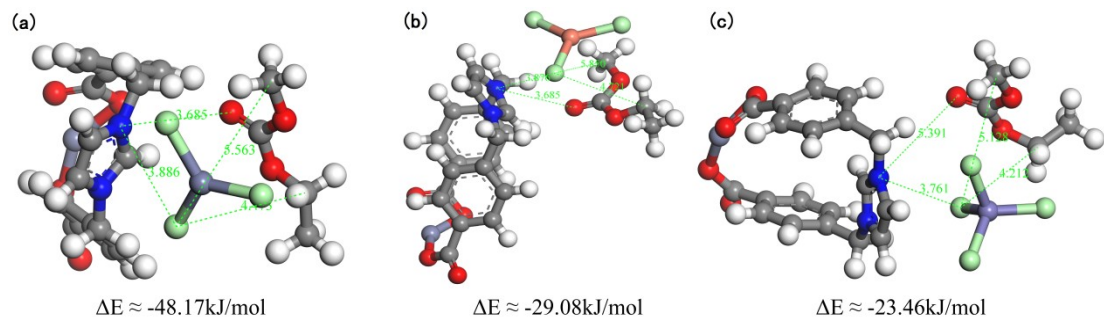


Fig. S4 Interaction energy between EMC and ILs

(a) IL-ZnCl₃-EMC; (b) IL-CuCl₃-EMC; (c) IL-FeCl₄-EMC;

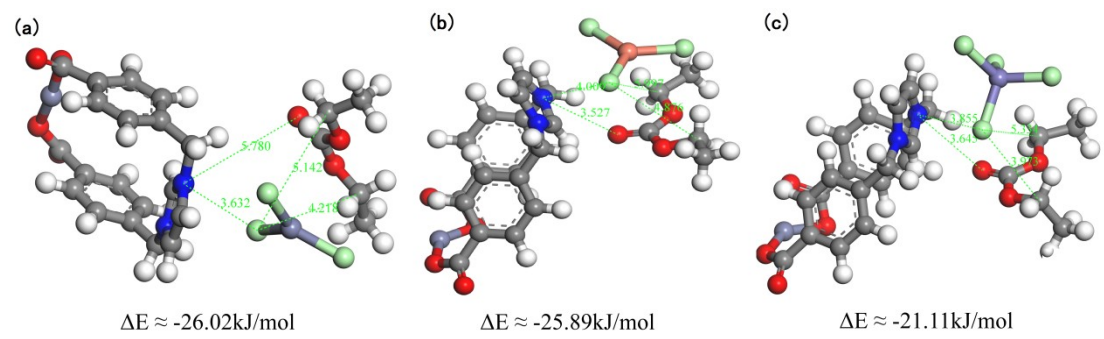


Fig. S5 Interaction energy between DEC and ILs

(a) IL-ZnCl₃-DEC; (b) IL-CuCl₃-DEC; (c) IL-FeCl₄-DEC

Tab. S1 Factors and Levels of (L_n3^4) orthogonal tests

	Temperature (A)(°C)	Pressure (B) (kPa)	Time (C) (min)	Catalyst dosage (D) (wt %)
1	165	2	20	0.2
2	175	4	40	0.4
3	185	6	60	0.6

Tab. S2 Effects of different process parameters on the catalytic process

No.	Factors				Conv. (%)	Yield (%)
	A(°C)	B(kPa)	C(min)	D(wt %)		
1	165 (1)	2 (1)	20 (1)	0.2 (1)	84.83	81.52
2	165 (1)	4 (2)	40 (2)	0.4 (2)	87.43	85.69
3	165 (1)	6 (3)	60 (3)	0.6 (3)	86.24	83.44
4	175 (2)	2 (1)	40 (2)	0.6 (3)	99.08	98.16
5	175 (2)	4 (2)	60 (3)	0.2 (1)	98.14	97.05
6	175 (2)	6 (3)	20 (1)	0.4 (2)	94.34	93.03
7	185 (3)	2 (1)	60 (3)	0.4 (2)	96.41	94.51
8	185 (3)	4 (2)	20 (1)	0.6 (3)	93.64	91.12
9	185 (3)	6 (3)	40 (2)	0.2 (1)	94.04	92.18
K_{j1}	258.5 /250.65	280.32/ 274.19	272.81 /265.67	277.01 /270.75	—	—
K_{j2}	291.56 /288.24	279.21/ 273.86	280.55 /276.03	278.18 /273.23	—	—
K_{j3}	284.09 /277.81	274.62/ 268.65	280.79 /275	278.96 /272.72	—	—
k_{j1}	86.17 /83.55	93.44 /91.40	90.94 /88.56	92.34 /90.25	—	—
k_{j2}	97.19 /96.08	93.07 /91.29	93.52 /92.01	92.73 /91.08	—	—
k_{j3}	94.70 /92.60	91.54 /89.55	93.60 /91.67	92.99 /90.91	—	—
R	11.02 /12.53	1.90 /1.85	2.66 /3.45	0.65 /0.83	—	—

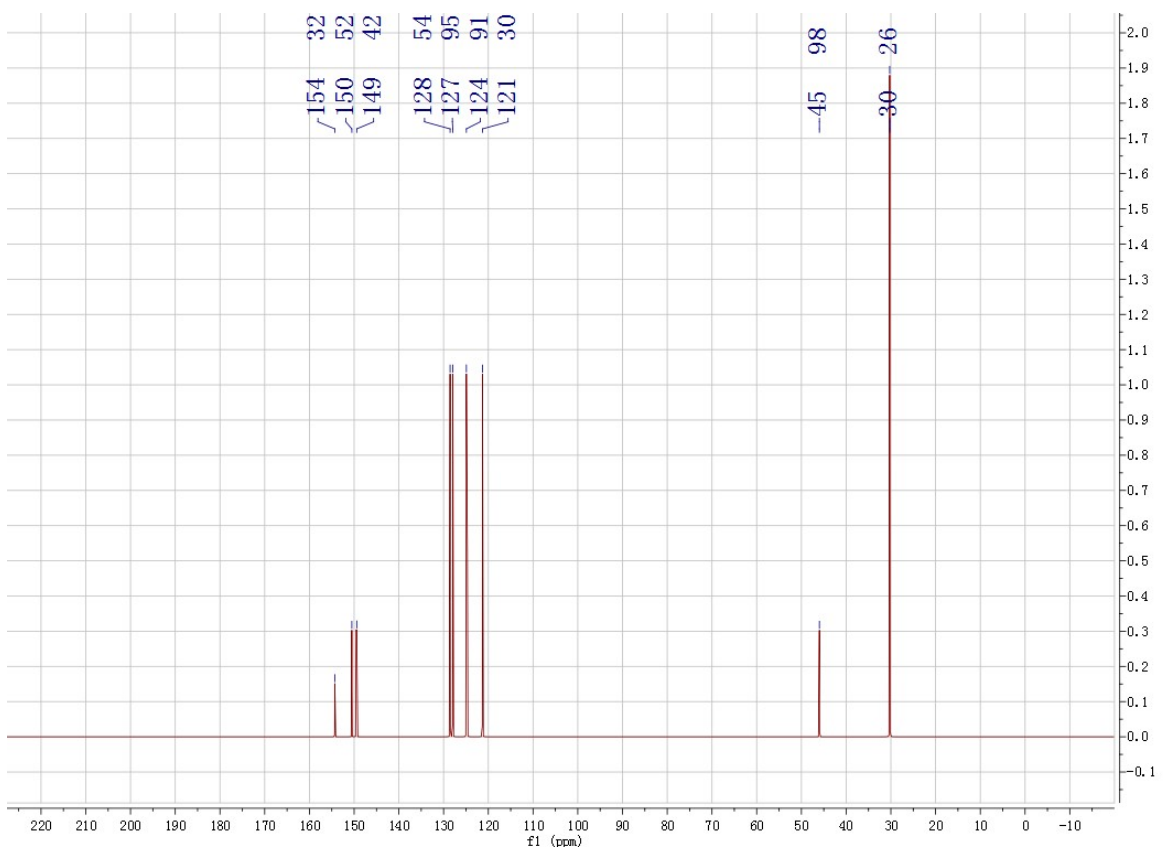


Fig. S6. ^{13}C -NMR of PIB-0 (150 MHz, CDCl_3).

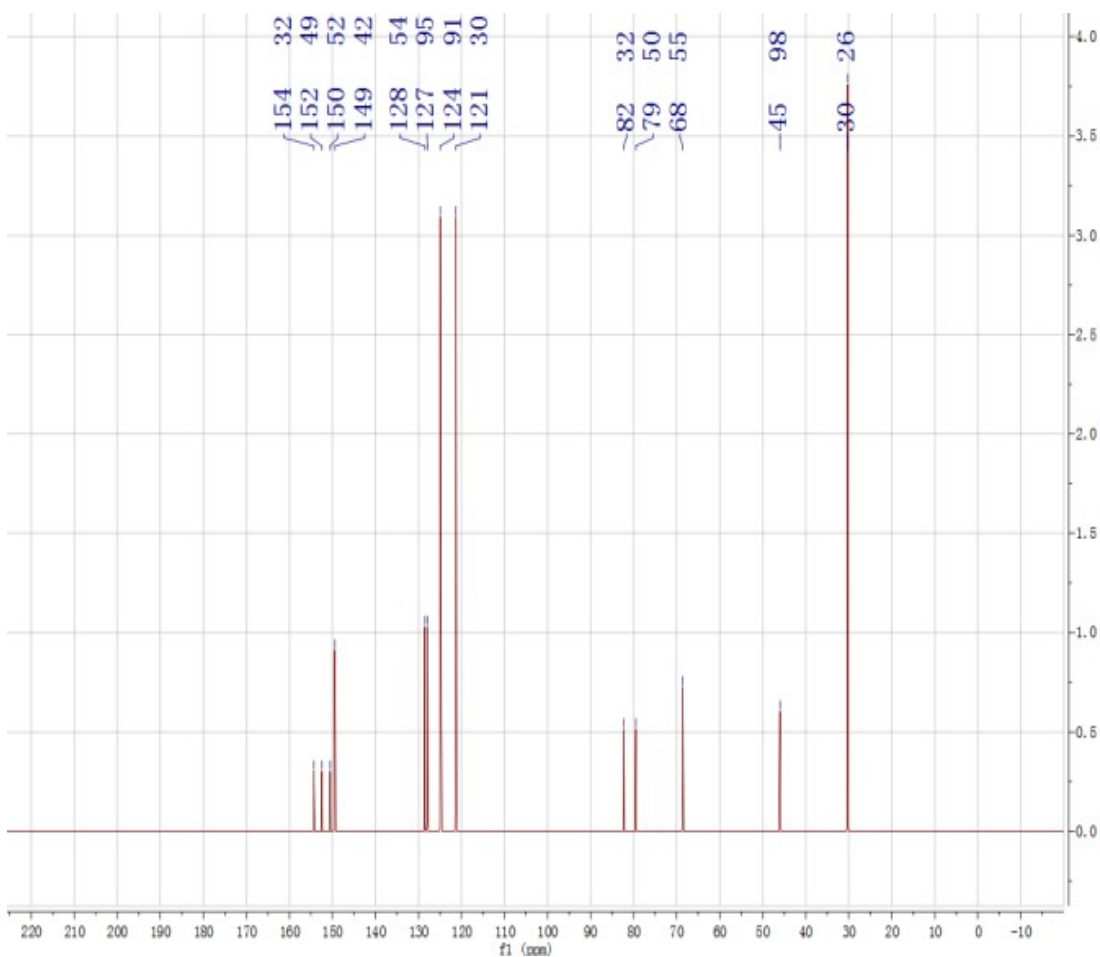


Fig. S7. ¹³C-NMR of PIB-30 (150 MHz, CDCl₃).

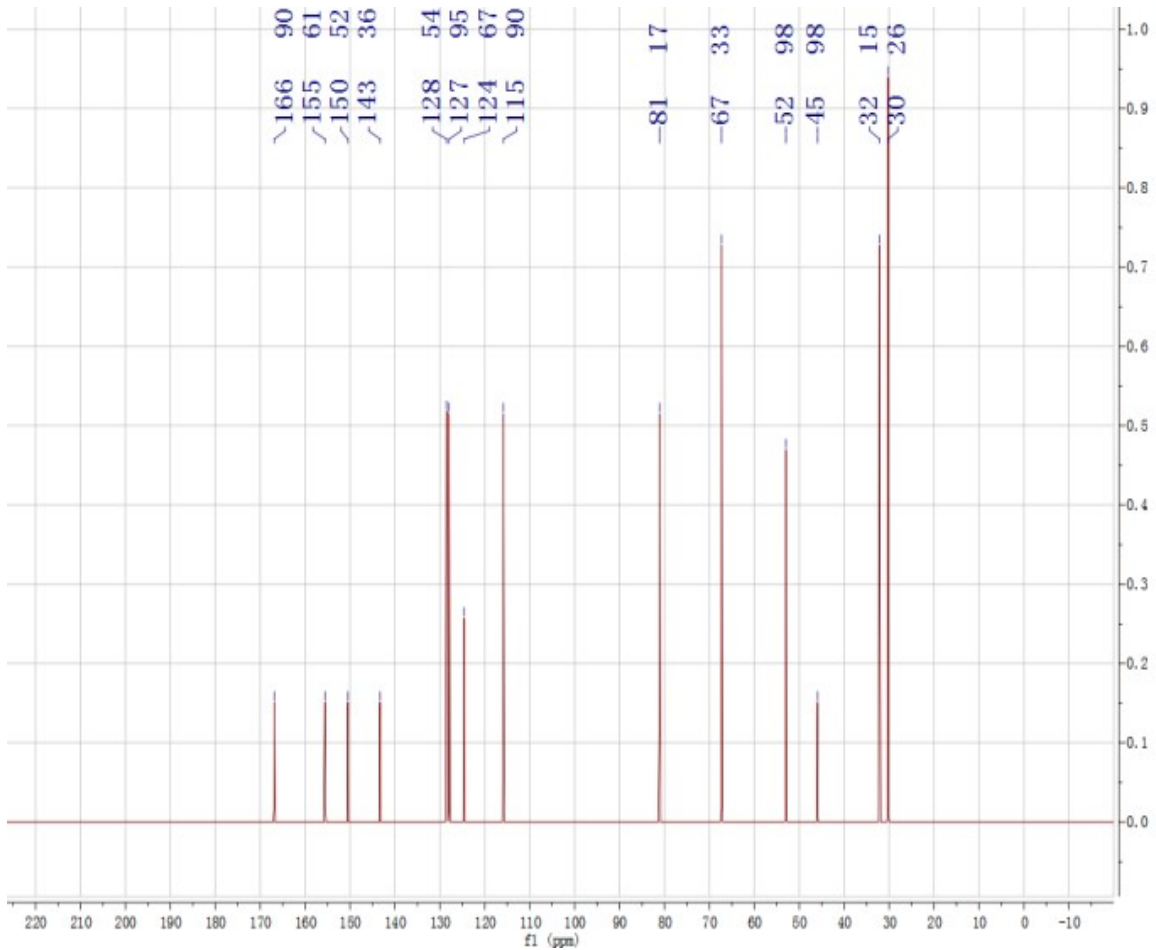


Fig. S8. ¹³C-NMR of PIB-50 (150 MHz, CDCl₃).

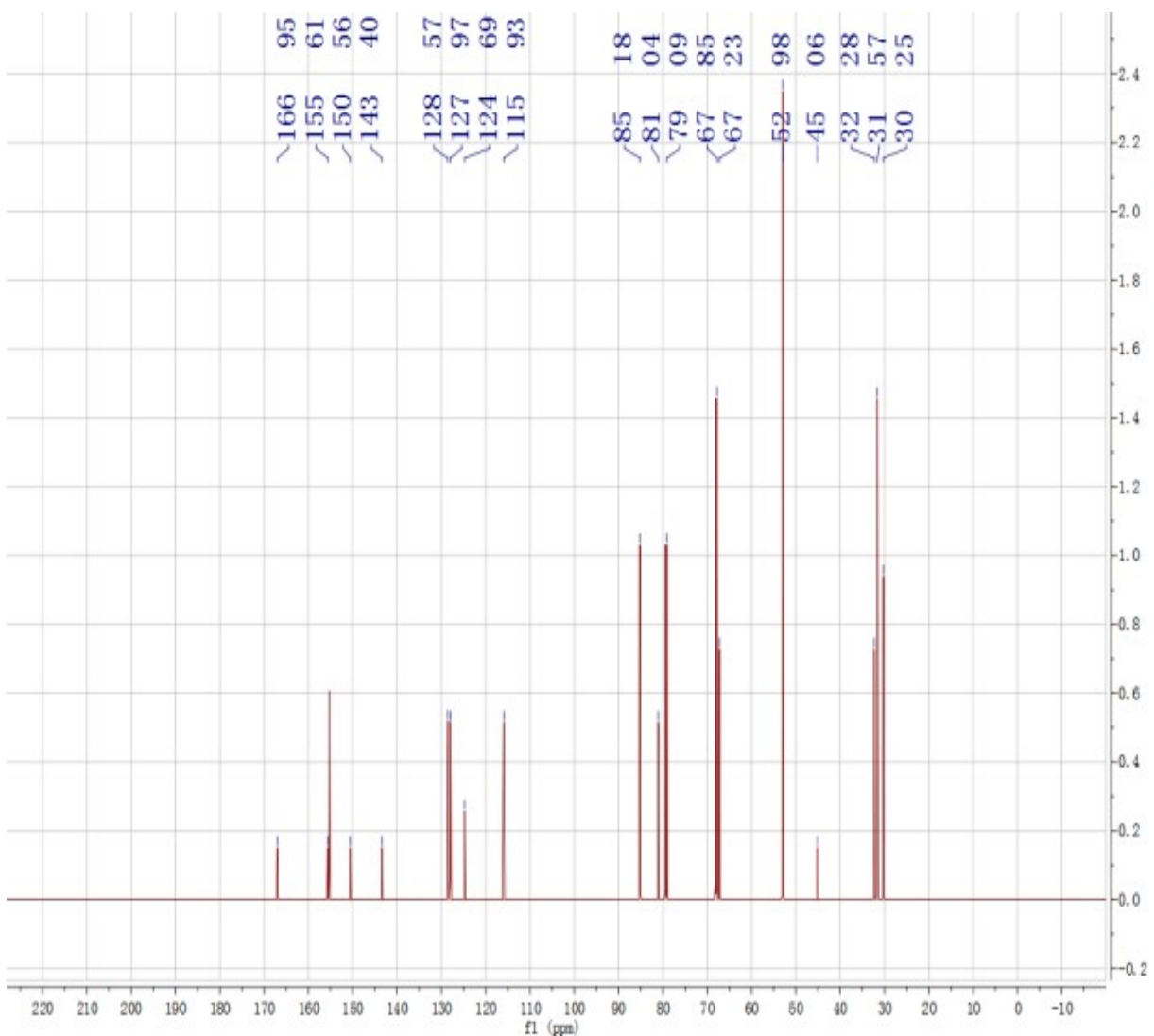


Fig. S9. ¹³C-NMR of PIB-70 (150 MHz, CDCl₃).

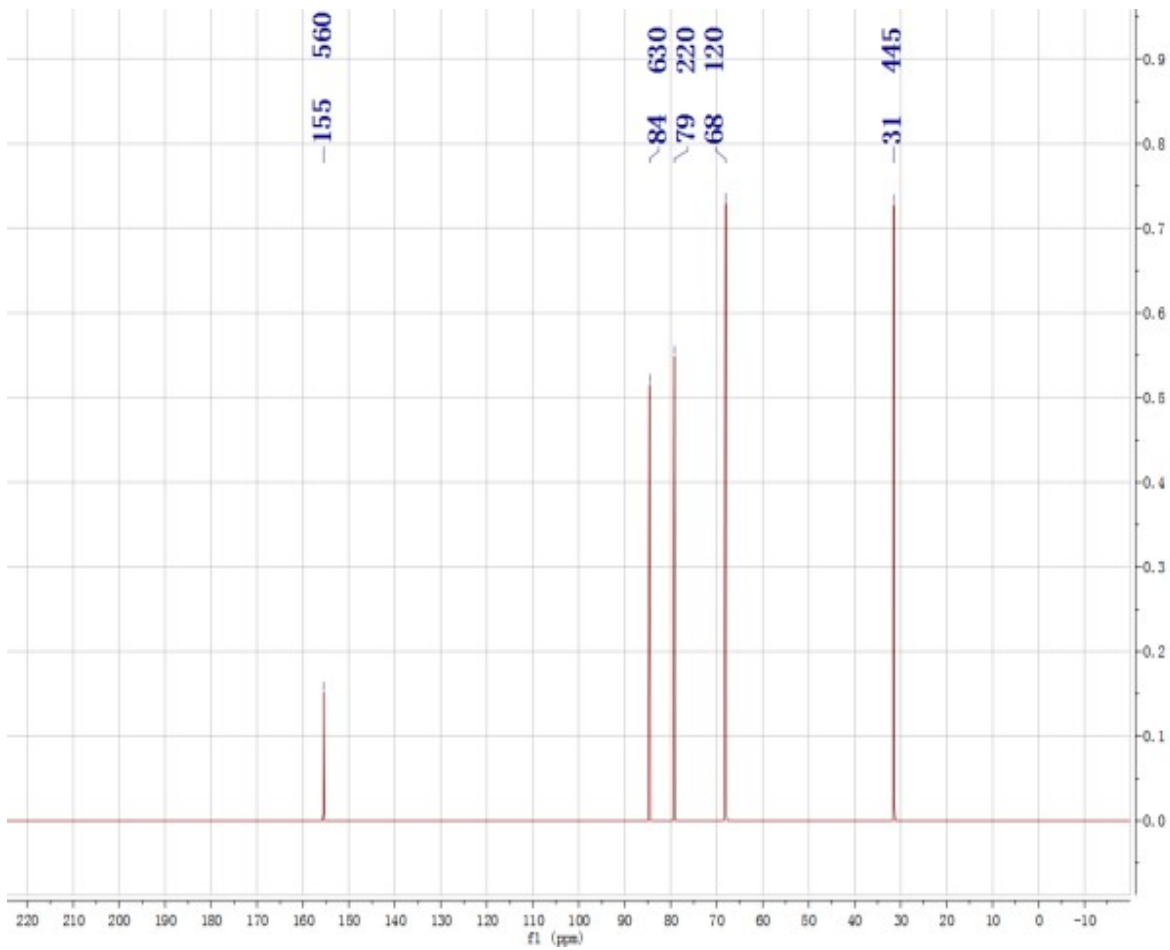


Fig. S10. ¹³C-NMR of PIB-100 (150 MHz, CDCl₃).

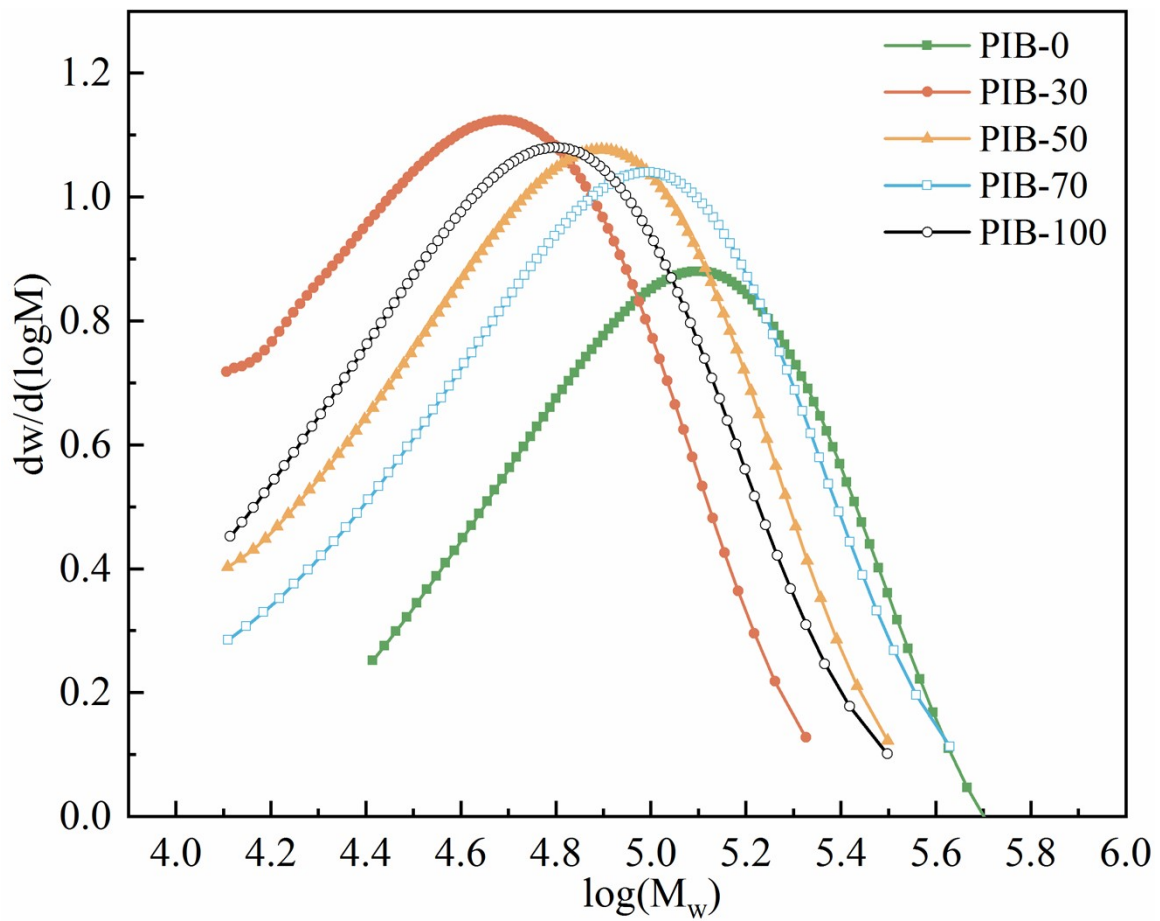


Fig. S11. GPC of copolymerised PIBs.



Fig. S12. Photo of stretching spline for injection molding

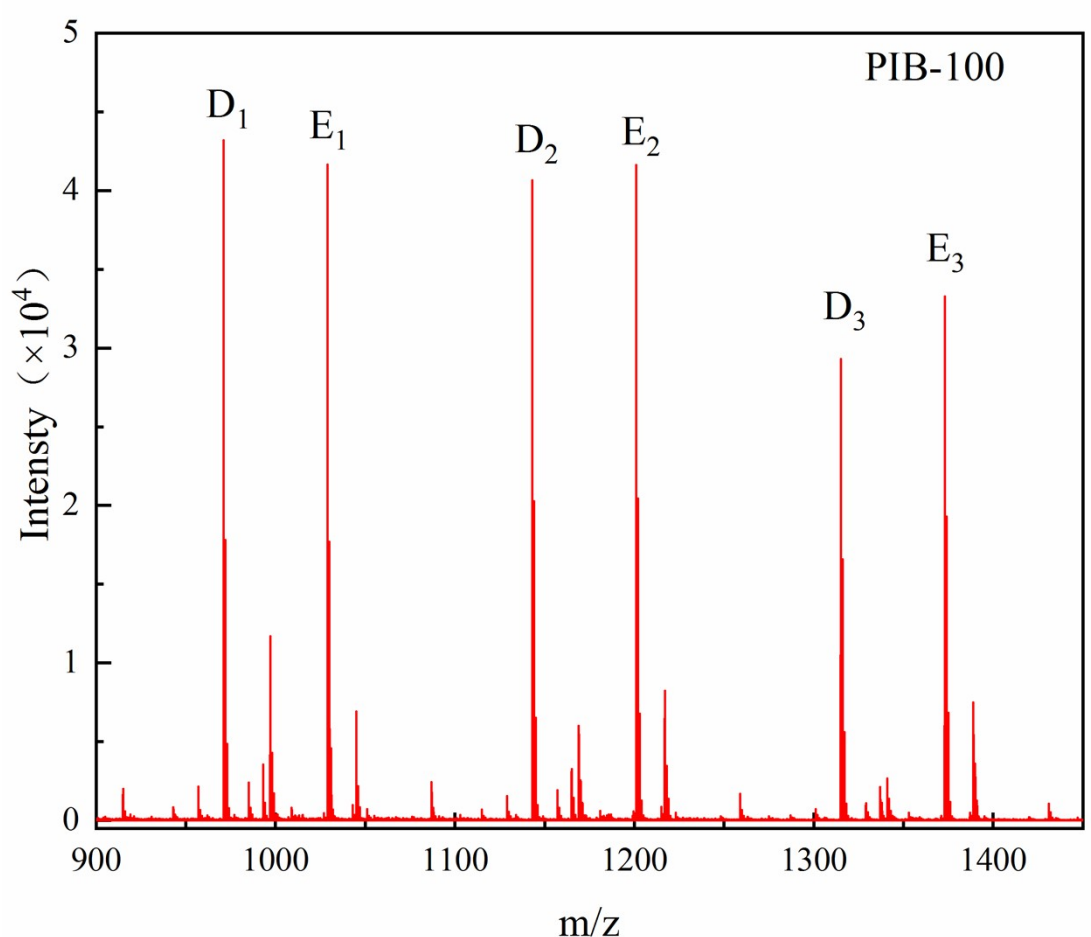
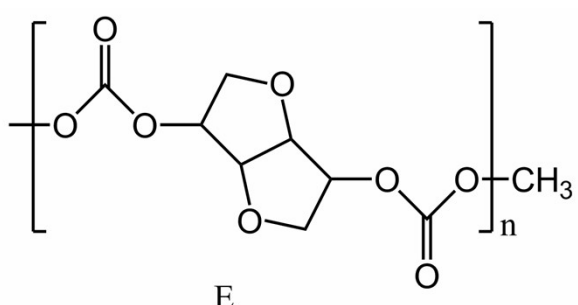
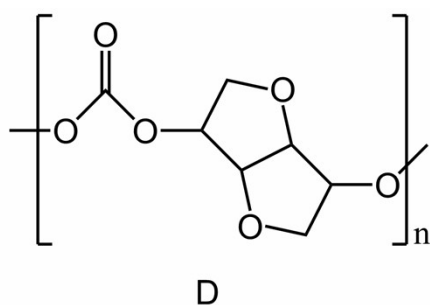


Fig. S13. The GPC profiles for the PIB-100 analyzed by the MALDI-TOF MS.

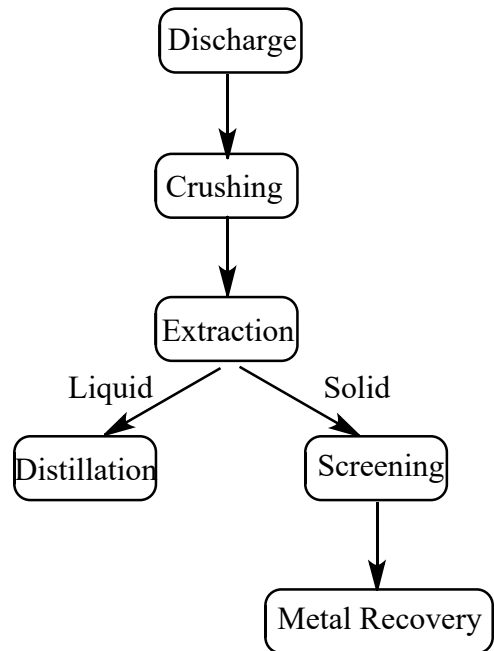


Fig. S14. Spent lithium battery recycling process

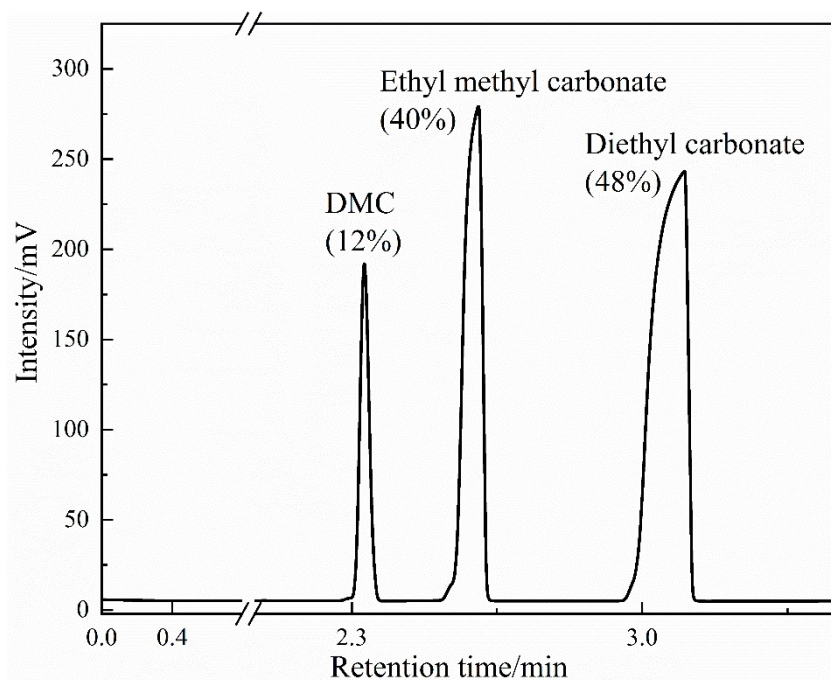


Fig. S15. Gas chromatography of s-LIBs